Cement & Concrete Composites 31 (2009) 699–704

Contents lists available at ScienceDirect

Cement & Concrete Composites

journal homepage: www.elsevier.com/locate/cemconcomp

Cracking behavior of concrete with shrinkage reducing admixtures and PVA fibers

Alexandra Passuello [a,*], Giacomo Moriconi [a], Surendra P. Shah [b]

[a] Department of Physics and Materials and Territory Engineering, Polytechnic University of Marche, AN 60131, Italy
[b] Center for Advanced Cement-Based Materials, Northwestern University, IL 60208, USA

ARTICLE INFO

Article history:
Received 14 May 2009
Received in revised form 14 August 2009
Accepted 18 August 2009
Available online 21 August 2009

Keywords:
Concrete
Shrinkage
Cracking
Shrinkage reducing admixtures
PVA fibers
Prediction of cracking

ABSTRACT

The reduction of the risk of cracking has been evaluated by the reduction of drying shrinkage due to the addition of shrinkage reducing admixtures (SRA) and by the increase of the crack opening resistance due to the addition of fibers. Both technologies have been considered individually and used in combination. It has been noted that the addition of SRA delays the time of cracking and the addition of fiber reduces the crack opening. However, the addition of the shrinkage reducing admixture (SRA) to the fiber-reinforced concrete has led the concrete to a better cracking behavior even when the fiber dosage had been reduced. Finally, the cracking time has been predicted by applying two different theoretical approaches.

1. Introduction

With proper mix-design and adequate construction process, that includes mixing, casting, vibration, and curing, concrete can be a reasonably durable material. However, even when all details are considered during the construction phase, if cracking appears on the concrete surface it can be a critical problem in terms of durability. The presence of cracks creates a free path for deleterious substances that may lead to premature deterioration and the reduction of the structure service life [1].

Restrained drying shrinkage can be a cause of cracking in concrete. The problem is the development of tensile stresses due to the movement restriction to which the concrete is submitted. Since concrete has low fracture resistance, in particular at early ages, very often, cracks do occur. Structures with low volume to surface area ratio are more vulnerable to the problem, and especially pavements and industrial floors that do not have formwork protection after casting.

Shrinkage reducing admixtures have been used to reduce the potential for shrinkage cracking [2–7]. The cracking reduction observed in concrete containing SRA is correlated to a lower rate of shrinkage and a reduction in the overall extent of shrinkage. On the other hand, fibers have been used to improve the cracking resistance of the brittle concrete matrix [8–10]. By transferring the stresses across the cracks, the fibers limit the crack width.

2. Research significance

Shrinkage reducing admixtures and fibers have been used to reduce the cracking potential of the concrete. These products have been previously analyzed independently, without considering their combination. However, in this study the reduction of cracking due to the addition of the SRA and fibers, used separately or in a blend, were investigated and analyzed.

Ring tests and free shrinkage tests were carried out to evaluate the cracking behavior of the concrete. Also, flexural test were carried out in order to obtain fracture parameters and tensile strength. Two different mathematical models were applied to predict the time of cracking in the mixtures without fibers. Finally, experimental results were compared with theoretical predictions.

3. Experimental investigation

3.1. Concrete composition

The experimental program involved the evaluation of six concrete mixtures, as shown in Table 1. The mixture proportion by weight was 1:2.1:2.1:0.5 (cement:sand:pea gravel:water) and it was kept constant for all mixtures. The difference between them is the presence or not of shrinkage reducing admixtures (SRA)

* Corresponding author. Tel.: +39 0422 774144.
E-mail address: passuelo@gmail.com (A. Passuello).

0958-9465/$ - see front matter © 2009 Elsevier Ltd. All rights reserved.
doi:10.1016/j.cemconcomp.2009.08.004

Table 1
Concretes mix proportions.

Materials	Concrete	1	2	3	4	5	6
		Plain	SRA	F200	F45	SRA F200	SRA F45
Cement	kg/m^3	400	400	400	400	400	400
Pea gravel	kg/m^3	840	840	840	840	840	840
Sand	kg/m^3	840	840	840	840	840	840
Water	kg/m^3	200	196	196	200	194	196
SRA	kg/m^3	–	4	–	–	4	4
PVA fiber	Type	–	–	Microfiber	Macrofiber	Microfiber	Macrofiber
	kg/m^3	–	–	6.50	6.50	3.25	3.25
	%*	–	–	0.50	0.50	0.25	0.25
Superplasticizer	kg/m^3	–	–	4	–	2	–

* By volume of concrete.

and fibers. In the water/cement value the liquid from SRA and superplasticizer was taken into account.

3.2. Materials

The cement used in this study was of type HS according to ASTM C 1157 [11] with a Blaine fineness of 502 m^2/kg. A Differential Thermal Analysis test identified that the cement had about 7.5% of limestone filler in its composition. Based on the mechanical properties obtained from the supplier and the dosage of limestone filler added to the clinker this cement could be classified as a type CEM II/LL 42.5R according to UNI–EN 197/1 [12], which is the most common cement type used in Italy. Pea gravel with 9.5 mm maximum aggregate size and a specific gravity of 2.65 was used. The sand was a dry natural river sand, having maximum a grain size of 4.5 mm and a specific gravity of 2.66. The shrinkage reducing admixture used in this study was a commercially available product (ECLIPSE FLOOR), mainly composed of propylene glycols. The dosage used was 1% by weight of cement. Only PVA fibers were used in this study. However, two different aspect ratios were analyzed. The PVA fibers show the same benefits as other synthetic fibers. Nevertheless, their tensile strength and elastic modulus are much higher than the synthetic ones and in addition the PVA fibers develop a very strong bond to the cement paste [13–15]. The mechanical and geometrical properties of both micro and macro PVA fibers used are shown in Table 2. To improve workability and allow a homogeneous dispersion of the PVA microfibers (F200), a polycarboxylate-based superplasticizer was added.

3.3. Mixing procedure and specimen preparation

The concrete batches were mixed in a laboratory vertical mixer. The aggregates and the cement were mixed with the whole amount of water for 2 min. Then, the chemical admixtures and fiber were gradually added to the respective mixtures, following this sequence: superplasticizer, shrinkage reducing admixtures and fibers. The total mixing time was 10 min, with three intermediate stops of 1 min each for scraping the wall and bottom of the drum and to clean the dry material that adhered to the wall and bottom.

All of the specimens were cast in the same way. Half of the mold was filled with concrete and vibration was applied manually, then the whole volume of the mold was filled and the vibration procedure was repeated. A steel trowel was used to finish the surface and then all the specimens were covered with a plastic sheet to prevent moisture loss. After 24 h from mixing, all the specimens were demolded and exposed to a standard environmental condition with a temperature of 23 ± 1 °C (73.4 ± 1.8 °F) and relative humidity of 50 ± 5%.

3.4. Tests methods

The ring test was performed to evaluate the cracking behavior of the concretes in restrained shrinkage conditions. The test was carried out following the suggestion of the standard ASTM C 1581–04 [16], however, some geometry modifications were made. As shown in Fig. 1, the thickness of the concrete ring (50 mm) used in this work was larger than that suggested by the ASTM standard (38 mm). This created a better situation for casting and vibration for the fiber-reinforced concrete using macrofibers. The height of the rings was 150 mm as suggested by the ASTM standards. Two

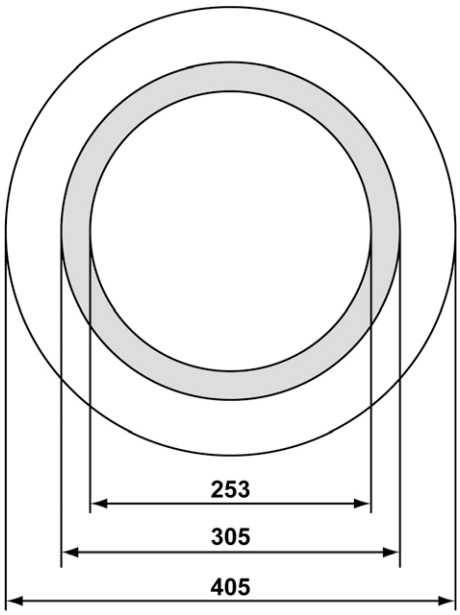

Fig. 1. Geometry of the ring test (dimensions in mm).

Table 2
Mechanical and geometrical properties of the PVA fibers.

Fiber	Length, L (mm)	Diameter, D (μm)	Aspect ratio (L/D)	Tensile strength (MPa)	Elastic modulus (MPa)	Elongation (%)
F200	8	40	200	1600	42,000	6
F45	30	660	45	900	23,000	7

ring specimens were cast for each concrete mixture. The specimens were cast around a steel ring, using a cardboard tube as an outside mold. Immediately after demolding the external cardboard ring, at the age of 1 day, the top surface of the ring specimens was sealed with silicone rubber. This procedure creates a condition that allows drying just from the outer circumferential surface, since the wooden base automatically seals the bottom surface of the concrete ring. Steel ring strain measurements were monitored from the casting time, having the subsequent readings taken every half-an-hour until the concrete ring cracked. After that, measurements of the cracking widths were taken every day for at least 2 weeks. A microscope with an accuracy of 0.01 mm was used to measure the widths. The results reported in this paper are the average of three measurements taken along the cracking length (top, center and bottom).

Free shrinkage measurements were performed on companion prismatic specimens ($100 \times 100 \times 300$ mm) of each concrete, using a length comparator according to ASTM C 157 [17]. Two layers of aluminum tape were used to seal the ends and two opposite faces of each prismatic specimen. This procedure was required to fix the volume-to-surface area ratio of both ring and prismatic specimens, which allowed comparison of free drying shrinkage.

Finally, for the concretes without fibers, flexural testing was performed according to a RILEM specification [18]. Three notched beam specimens ($50 \times 100 \times 450$ mm) were tested at five different ages (1, 3, 7, 14 and 28 days). The notch length was one-third of the beam depth and the specimens were cut immediately before testing. The beams were tested using a digitally controlled closed-loop hydraulic testing machine. The specimens were loaded using crack mouth opening displacement (CMOD) control at a constant rate of 0.0075 mm/min. After reaching the peak load, when the load was about 95% of the peak value, the specimens were unloaded and, then, reloaded.

4. Experimental results and discussion

4.1. Shrinkage cracking behavior

4.1.1. Effect of SRA

Fig. 2 shows the results of the strain measured at the steel ring for plain and SRA mixtures. In comparison with the plain concrete, the SRA mixture shows a lower strain during the ring test. This strain relaxation is the consequence of the lower total shrinkage and the lower development rate of the shrinkage obtained for this mixture, as shown in Fig. 3. The decrease of shrinkage allows the concrete to develop its mechanical properties, leading to a delay of the cracking time by about 10 days. The crack width developed in the SRA concrete ring showed an initial reduction of 30%, as reported in Fig. 4, and the small decrease in the rate of width growth in the SRA mixture led to a final crack width reduction of about 40%.

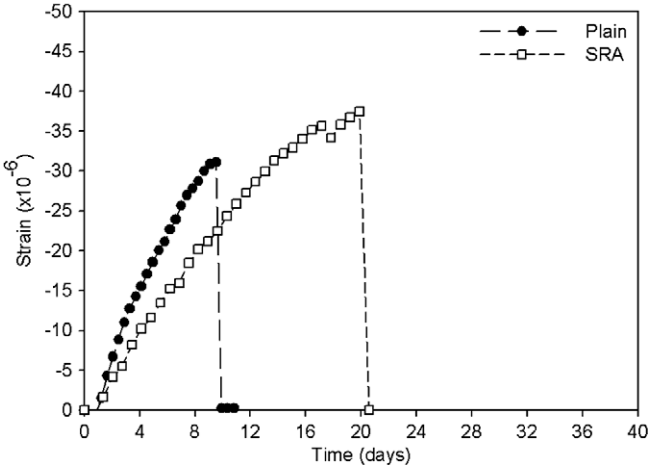

Fig. 2. Steel ring strain measurements for Plain and SRA concretes.

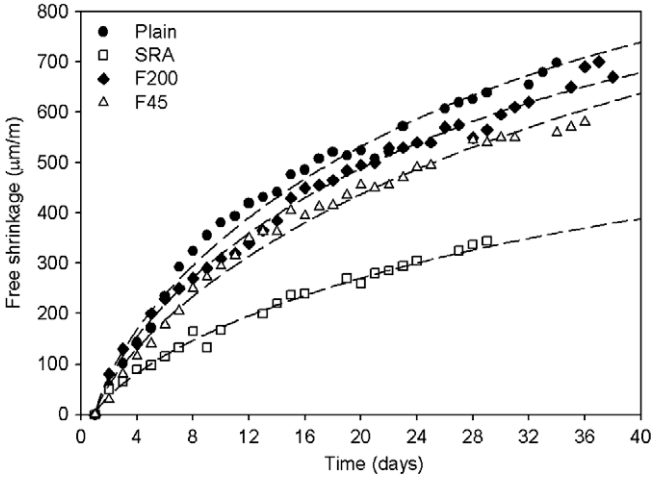

Fig. 3. Free shrinkage results.

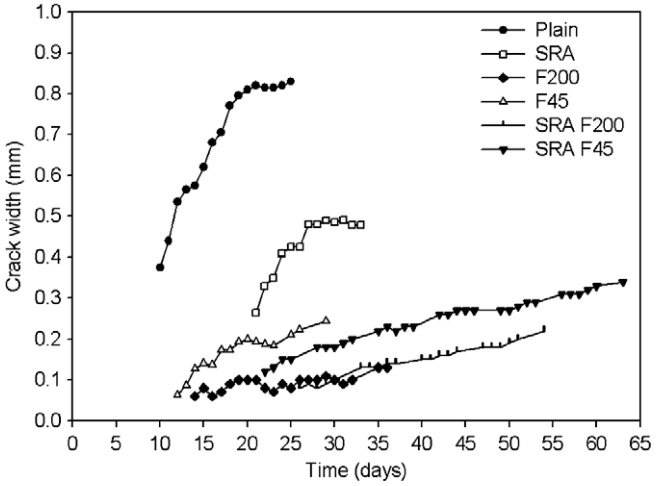

Fig. 4. Cracking widths during the exposure time.

4.1.2. The effect of fibers

As shown in Fig. 3, a small reduction of the free shrinkage was identified in both micro (F200) and macro (F45) PVA fiber-reinforced concrete. Usually, the fibers do not change the concrete shrinkage, however, in this work this behavior was observed for all specimens tested. Similar behavior has been reported by Sun et al. [19], especially when macrofibers were used. This may happen because the presence of fibers could modify the internal water movements within the concrete.

Nevertheless, the decrease observed for the free shrinkage tests was not enough to relax the strain in the steel ring, as shown in Fig. 5. In the literature, it is understood that the cracking behavior is related to the matrix of the concrete and the presence of the fibers should not modify the time that the first crack appears. Since the strain measured at the steel ring was basically the same for the plain and the fiber-reinforced concrete, the same cracking age should be expected for all mixtures. On the other hand, the fiber-

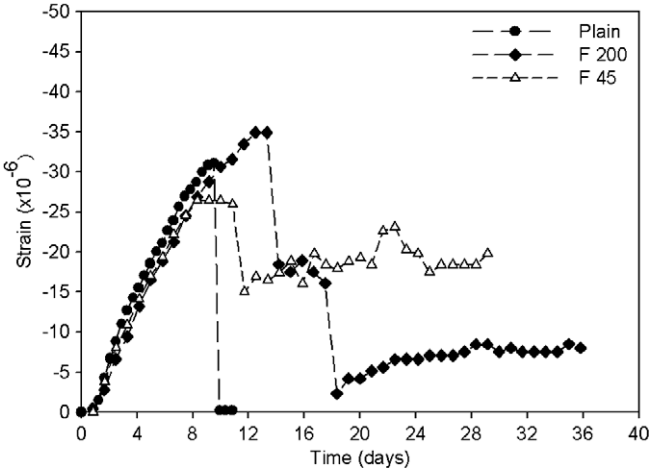

Fig. 5. Strain measurements of the steel ring for Plain and fiber-reinforcement concretes without SRA.

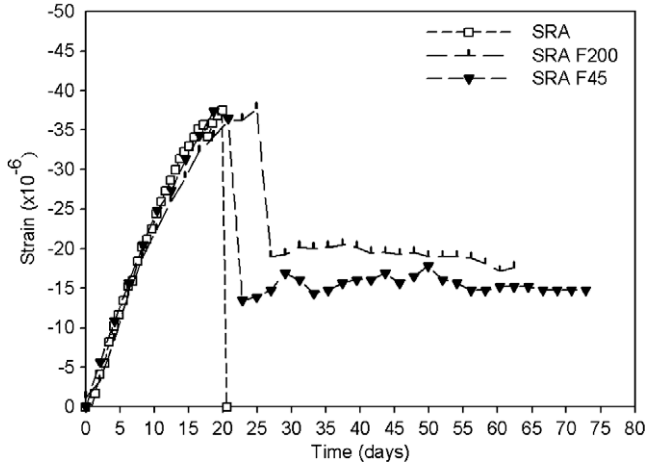

Fig. 6. Strain measurements of the steel ring for SRA and fiber-reinforced concretes with SRA.

reinforced concrete with the PVA microfibers showed a delay of about 4 days. Kim et al. [20] observed the same delayed behavior induced by fibers on the age of cracking.

Kwon et al. [21] explained the fracture behavior in drying restrained tests. Drying usually induces systems of parallel cracks near the surface exposed to air. As the drying front moves inside the concrete material, crack propagation and crack opening are concentrated into some of the initial cracks in a systematic manner. Parts of the microcracks continue to open over time, while others stop opening or start to close. In the plain concrete, there is no resistance against the propagation and only one crack is found to be completely formed. However, in the fiber-reinforced concrete, the weakest point of the matrix may change with time because of the fiber distribution. This could lead to a slight delay of the cracking time, as was observed in the fiber-reinforced concrete with the PVA microfibers. On the other hand, the fiber-reinforced concrete with the PVA macrofibers did not show the same behavior. This occurred because of the large size of these fibers, which doesn't allow a good stress transfer at a microcracking level.

Concerning the reduction of the crack width, the fibers are much more effective than SRA. As shown in Fig. 4, both PVA micro (F200) and macrofibers (F45) reduced the width by more than 90% at the moment the crack appeared. The difference shown between them was the opening rate of the crack width. The PVA microfibers maintained, during this time, nearly the same crack width, with a very low opening rate. In fact, the small geometry and the larger number of fibers in the concrete increase the surface area in contact with the concrete matrix. This allows a better stress transfer across the cracking and better crack opening control.

For the microfiber reinforced concrete (F200), a second crack was identified 4 days after the first one appeared. The presence of more than one crack in the fiber-reinforced concrete is an expected result, since the fibers create internally several small restraints on the concrete. The presence of several cracks limits the crack widths, since the crack opening is shared between all of them.

4.1.3. The effect of the SRA/fibers blended

Fig. 6 shows the strain results of the mixtures containing both shrinkage reducing admixture and fibers. The strain measurements for the fiber-reinforced concrete with SRA were basically the same as those observed in the SRA mixture without fibers. It was supposed that the fibers could not produce any further decrease in the free shrinkage in SRA concretes and for this reason free shrinkage tests were not carried out with these mixtures.

The presence of SRA in the fiber-reinforced concrete did not modify the cracking time behavior from that observed in the case where the SRA was used separately. Basically, the delay of the cracking time observed in these blended mixtures was due to the presence of the SRA.

With respect to the opening of the crack width, Fig. 4 shows interesting results for the SRA/Fibers blend. When SRA was added, the same cracking behavior was observed in spite of a much lower fiber dosage. Moreover, other than the microfiber reinforced concrete without SRA, the SRA/PVA microfiber blend showed just one crack without any crack width increase.

In the case of the macrofibers mixtures, the presence of SRA led to a further reduction of the cracking width. These results are very important because the addition of a lower dosage of fibers is easier to process and less expensive to produce, resulting in a concrete mixture with good cracking behavior.

4.2. Prediction of cracking

The prediction of cracking was made only for the concretes without fibers. It was based on the comparison of two different theoretical methods. It is important to notice that in this work calculations have not considered the stresses caused by the humidity profile [22–24] that developed in the concrete ring.

The first applied model was proposed by Shah et al. [25] and automated by Weiss et al. [6]. It is based on the fracture mechanics concepts with consideration of the energy balance. The energy requirement for unstable crack growth, according to this method, is represented the following equation:

$$G \geq R \tag{1}$$

In the equation above, G is the strain energy release rate that depends on the crack length (G-curve), while R is the fracture resistance, which means the consumed energy rate (R-curve). A full explanation of the approach and the equations used in this method can be found elsewhere [25].

The R-curve used was based on the ring geometry. It is related to the cracking length and the material parameters K_{IC} and $CTOD_c$ that were obtained in the flexural tests [18]. Whereas the G-curve is related to the modulus of the concrete and the stress intensity factor (K_{IC}) for the ring specimen.

The prediction of cracking was made by comparing the maximum allowable shrinkage to the residual shrinkage – Fig. 7a and b. The maximum allowable shrinkage is directly obtained applying the condition $G \geqslant R$. On the other hand, the residual shrinkage is

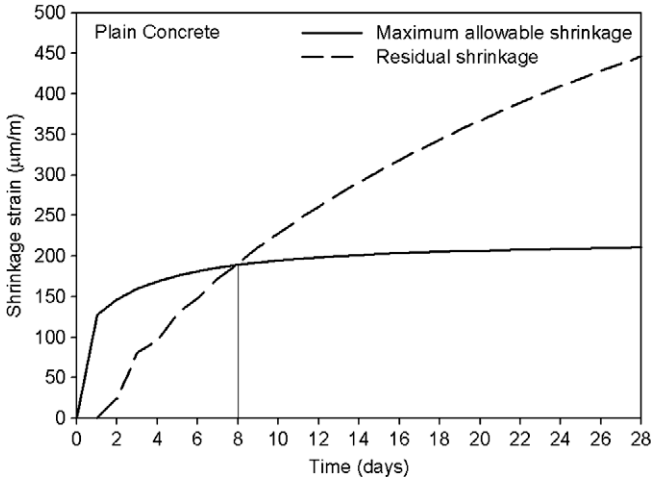

Fig. 7a. Results of the cracking prediction for plain concrete using the fracture model.

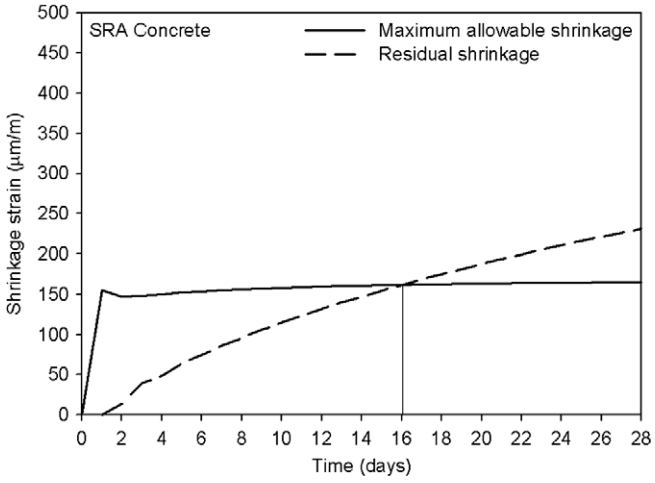

Fig.7b. Results of the cracking prediction for SRA concrete using the fracture model.

obtained from the free shrinkage results after creep considerations. In this study, the creep strains were approximated using the Comité Euro-International du Beton approach [6]. A full explanation about how to predict the creep can be found elsewhere [26].

The results obtained can be found in Fig. 7a and b. The fracture model predicted cracking times of 8 and 16 days for the plain and SRA concretes. These predictions are very close to the experimental results, which were 10 and 20 days, respectively.

The second method applied is based on the maximum tensile strength approach. According to this method, the crack appears at the moment that the tensile stress, developed by the restrained shrinkage, reaches the maximum tensile strength of the concrete. The cracking requirement is represented the following equation:

$$\sigma_{residual} \geq f_{tensile} \quad (2)$$

The prediction of cracking was made with the comparison between the concrete tensile strength ($f_{tensile}$) and the residual tensile stress ($\sigma_{residual}$) – Fig. 8a and b. The concrete tensile strength was calculated from 60% of the flexural strength obtained from the flexural tests [18], as suggested by Collepardi [13]. The residual tensile stress is that expected due to the restrained shrinkage. It was calculated using the free shrinkage results after creep considerations. The equations to calculate the theoretical tensile stress can be

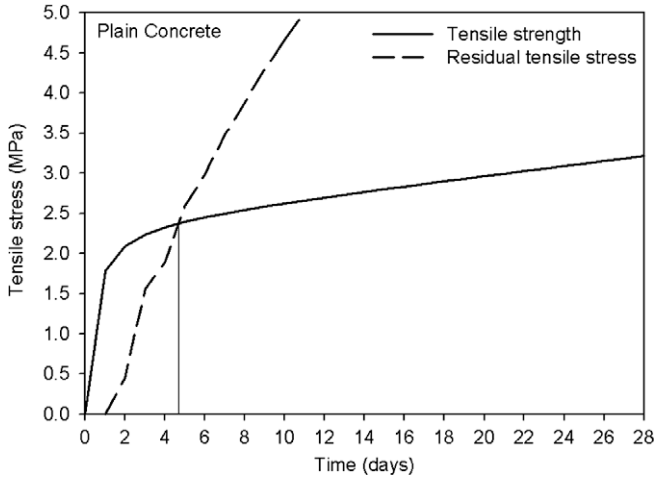

Fig. 8a. Results of the cracking prediction for plain concrete using the tensile strength model.

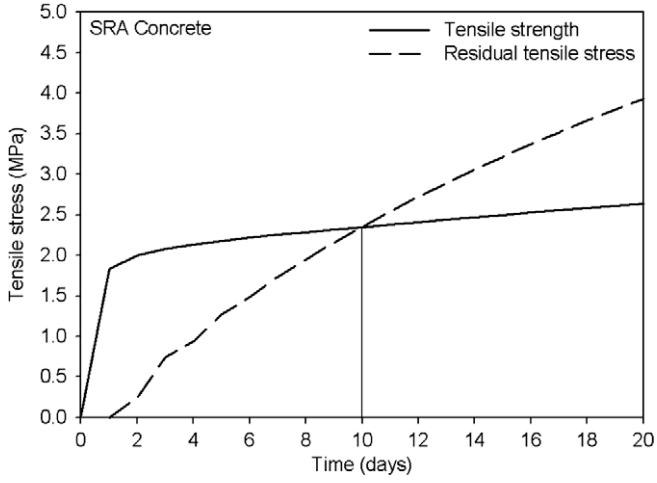

Fig. 8b. Results of the cracking prediction for SRA concrete using the maximum tensile model.

found elsewhere [27]. The results obtain are shown in Fig. 8a and b. Using the maximum tensile strength model, cracking should occur after 4 and 10 days for the plain and SRA concretes. These cracking times are rather far from the 10 and 20 days obtained in the experimental tests.

The better cracking predictions showed that the fracture model could be related to the quasi-brittle behavior of the concrete. In brittle materials, the cracking instability is observed when the tensile strength is reached. However, in the concrete a stable crack growth occurs prior to the peak stress and strain softening is observed in the postpeak region. It could explain why the cracking has not appeared when the tensile strength is reached. On the other hand it is important to notice that the tensile strength was obtained from the flexural test and for this reason we should expect a certain variability of the results. Also, the tensile strength was calculated using 60% of the flexural strength as suggested by Collepardi [13]. If the 80% recommended by ACI [28] were used instead, the maximum tensile model would match better with the experimental results.

5. Conclusions

It has been noted that the addition of SRA delays the time of cracking, reducing the crack width by 40%. The addition of fibers,

on the other hand, does not greatly modify the cracking time, but does reduce the crack width by about 70% in the case of macrofibers, and by almost 90% with microfibers. The addition of shrinkage reducing admixture (SRA) to the fiber-reinforced concrete produced a better cracking behavior, even when the fiber dosage had been reduced. Finally, the cracking time has been predicted for the concretes without fibers by applying two different theoretical approaches. The experimental results obtained in this work have better matched the cracking predictions obtained with the model based on fracture mechanics.

Acknowledgements

The authors gratefully acknowledge support received from the University of Marche (UNIVPM), ENCO srl, and the Center for Advanced Cement-Based Materials (ACBM). Also, the support of Grace Construction Products, Holcim (US) Inc., and Kuraray Group is greatly appreciated.

References

[1] Collepardi M. The New Concrete, prima edizione. Tintoretto 2006. p. 421.
[2] Weiss J, Berke N. Admixtures for reduction of shrinkage and cracking, early age cracking in cementitious systems – state of the art report. Bentur A, in press. [chapter 7.5].
[3] Shah SP, Weiss WJ, Yang W. Shrinkage cracking – can it be prevented? Concr Int 1998;20(4):51–5.
[4] Gettu R, Roncero J, Martin MA. Study of the behavior of concrete with shrinkage reducing admixtures subjected to long-term drying. ACI-Spec Publ Concr: Mater Sci Appl 2002;206:p. 157–166.
[5] Shah SP, Karaguler ME, Sarigaphuti M. Effects of shrinkage reducing admixtures on restrained shrinkage cracking in concretes. ACI Mater J 1992;89(3):p. 288–290.
[6] Weiss WJ, Shah SP. Shrinkage cracking of restrained concrete slabs. J Eng Mech 1998;124(7):p. 765–774.
[7] Brooks JJ, Jiang X. The influence of chemical admixtures on Restrained Drying Shrinkage of Concrete. ACI SP-173 – chemical admixtures. 1994:p. 249–265.
[8] Voigt T, Bui VK, Shah SP. Drying shrinkage of concrete reinforced with fibers and welded-wire fabric. ACI Mater J 2004;101(3):p. 233–241.
[9] Betterman LR, Ouyang C, Shah SP. Fiber-matrix interaction in microfiber-reinforced mortar. Adv Cem Based Mater 1995;2:p. 53–61.
[10] Banthia N, Yan C, Mindess S. Restrained shrinkage cracking in fiber reinforced concrete: a novel test technique. Cem Concr Res 1996;26(1):p. 9–14.
[11] ASTM C 1157. Standard performance specification for hydraulic cement; 2008.
[12] UNI_EN 197/1. Cemento – parte 1: composizione, specificazioni e criteri di conformità per cementi comuni; 2006.
[13] Collepardi M. Il Nuovo calcestruzzo, terza edizione. Tintoretto 2003:p. 391.
[14] Zheng Z, Feldman D. Synthetic fibre-reinforced concrete. Prog Polym Sci 1995;20:p. 185–210.
[15] Garcia S, Naaman AE, Pera J. Experimental investigation on the potential use of poly(vinyl alcohol) short fibers in fiber-reinforced cement-based composites. Mater Struct 1997;30(January–February):p. 43–52.
[16] ASTM C 1581-04. Standard test method for determining age at cracking and induced tensile stress characteristics of mortar and concrete under restrained shrinkage; 2004.
[17] ASTM C 157/C 157M – 06. Standard test method for length change of hardened hydraulic-cement mortar and concrete.
[18] RILEM Committee on Fracture Mechanics of Concrete – Test Methods. Determination of the fracture parameters (K_{IC} and $CTOD_c$) of plain concrete using three-point bend tests. Mater Struct 1990;23(6):457–60.
[19] Sun W, Chen H, Luo X, Qian H. The effect of hybrid fibers and expansive agent on the shrinkage and permeability of high-performance concrete. Cem Concr Res 2001;31:p. 595–601.
[20] Kim B, Weiss J. Using acoustic emission to quantify damage in restrained fiber-reinforced cement mortars. Cem Concr Res 2003;33(2):p. 207–214.
[21] Kwon SH, Ferron RP, Akkaya Y, Shah SP. Cracking of fiber-reinforced self-compacting concrete due to restrained shrinkage. Int J Concr Struct Mater 2007;1(1):p. 3–9.
[22] Hossain AB, Weiss J. Assessing residual stress development and stress relaxation in restrained concrete ring specimens. Cem Concr Compos 2004;26:p. 531–540.
[23] Moon JH, Rajabipour F, Weiss J. Incorporating moisture diffusion in the analysis of the restrained ring test. In: Oh BH, et al., editors. Concrete under Severe Conditions: Environment & Loading, CONSEC'04, Seoul Korea; 2004. p. 12-34.
[24] Radlinska A, Moon JH, Rajabipour F, Weiss J. The ring test: a review of recent developments volume changes of hardening concrete. Lyngby, Denmark; 2006:p. 20–23.
[25] Shah SP, Ouyang C, Marikunte S, Yang W, Giraudon EB. A method to predict shrinkage cracking of concrete. ACI Mater J 1998;95(4):p. 339–346.
[26] Muller HS. New prediction models for creep and shrinkage of concrete ACI SP 135-1. Am Concr Inst Detroit 1994:p. 1–19.
[27] Moon JH, Weiss J. Estimating residual stress in the restrained ring test under circumferential drying. Cem Concr Compos 2006;28:p. 486–496.
[28] American Concrete Institute. Building code requirements for structural concrete and commentary (ACI-318-05), ACI Committee 318. 2005. p. 430.